DMD Fast Forward. Published on May 26, 2005 as doi:10.1124/dmd.105.004788

DMD #4788

Enantioselective Metabolism and Cytotoxicity of *R*-Ifosfamide and *S*-Ifosfamide by Tumor Cell-expressed Cytochromes P450*

Chong-Sheng Chen, Youssef Jounaidi and David J. Waxman+

Division of Cell and Molecular Biology,

Department of Biology, Boston University, Boston, Massachusetts 02215 (CSC, YJ, DJW)

DMD #4788

Running title – P450 activation of oxazaphosphorines

Corresponding author:
+ To whom correspondence should be addressed at:
Department of Biology
Boston University
5 Cummington Street
Boston, MA 02215
Fax: 617-353-7404
email: djw@bu.edu

Number of text pages: 28
3 Tables
3 Figures
40 Refs
242 Words in Abstract
548 Words in Introduction
1103 Words in Discussion

Abbreviations: P450 or CYP, cytochrome P450; P450R, P450 reductase; CAA, chloroacetaldehyde; CPA, cyclophosphamide; IFA, ifosfamide; FBS, fetal bovine serum; *N*-deCl, *N*-dechloroethylation; EC_{50}, effective drug concentration for 50% maximal response; IRES, internal ribosome entry site; PBS, phosphate-buffered saline.

Summary - The anti-cancer prodrug ifosfamide (IFA) contains a chiral phosphorous atom and is administered in the clinic as a racemic mixture of *R*-IFA and *S*-IFA. Hepatic cytochrome P450 (CYP) enzymes exhibit enantioselective preferences in the metabolism of *R*-IFA and *S*-IFA, however, the impact of this selectivity on P450-dependent anti-cancer activity is not known. Presently, the metabolism and cytotoxicity of *R*-IFA and *S*-IFA were determined in 9L gliosarcoma and CHO tumor cells expressing an IFA-activating P450 enzyme and by in vitro steady-state kinetic analysis using cDNA-expressed P450 enzymes. Tumor cells expressing CYP3A4 were the most sensitive to *R*-IFA cytotoxicity, whereas tumor cells expressing CYP2B1 or CYP2B6 were most sensitive to cyclophosphamide (CPA), an isomer of IFA. Correspondingly, CYP3A4-expressing cells and cDNA-expressed CYP3A4 metabolized *R*-IFA to yield the active, 4-hydroxylated metabolite at a 2 to 3-fold higher rate than *S*-IFA or CPA metabolism. CYP2B cells and cDNA-expressed CYP2B enzymes metabolized CPA almost exclusively by 4-hydroxylation, whereas *R*-IFA and *S*-IFA were substantially converted to inactive, *N*-dechloroethylated metabolites. Further investigation revealed that CYP3A1, a rat enzyme, exhibited superior kinetic properties compared to the human enzyme, CYP3A4, with *R*-IFA and *S*-IFA both metabolized with high catalytic efficiency by 4-hydroxylation and with a K_m of 200 μM, ~5-fold lower than CYP3A4. Based on these kinetic parameters and metabolic profiles, *R*-IFA is expected to exert greater anti-cancer activity than *S*-IFA or CPA against tumors that express CYP3A enzymes, whereas tumors expressing CYP2B enzymes may be more sensitive to CPA treatment.

DMD Fast Forward. Published on May 26, 2005 as DOI: 10.1124/dmd.105.004788
This article has not been copyedited and formatted. The final version may differ from this version.

Introduction

Ifosfamide (IFA) and its structural isomer cyclophosphamide (CPA) are clinically effective anti-cancer alkylating agent prodrugs used to treat a broad range of neoplasms. Both prodrugs are activated in the liver by a cytochrome P450-catalyzed 4-hydroxylation reaction. The primary 4-hydroxy metabolite exists in equilibrium with the ring-opened aldo(iso)phosphamide, which undergoes β-elimination to yield the therapeutically active, DNA cross-linking (iso)phosphoramide mustard and acrolein, a reactive aldehyde (Sladek, 1988; Zalupski and Baker, 1988). An alternative, P450-catalyzed *N*-dechloroethylation reaction inactivates the parent drug and generates the neurotoxic and nephrotoxic byproduct chloroacetaldehyde (CAA). Although CPA and IFA are very similar in chemical structure and mechanism of action, they differ strikingly with respect to their pharmacokinetic and pharmacodynamic properties. CPA is metabolized predominantly by 4-hydroxylation, catalyzed by CYP2B and CYP2C enzymes, whereas IFA undergoes extensive *N*-dechloroethylation catalyzed by CYP2B and CYP3A enzymes (Huang and Waxman, 1999; Roy et al., 1999b; Chen et al., 2004). The formation of CAA as a major byproduct of IFA *N*-dechloroethylation is associated with the neurotoxicity and urotoxicity seen in patients treated with IFA, but not in the case of CPA. These side effects can be controlled by administration of protective agents such as sodium 2-mercaptoethanesulfonate (Woodland et al., 2000).

IFA is a chiral molecule that contains an asymmetric phosphorus atom and exists in two enantiomeric forms, *R*-IFA and *S*-IFA. Studies in experimental animal models and human clinical trials indicate that the racemic IFA used in the clinic is subject to enantioselective metabolism, which may lead to distinct efficacies and toxicity profiles for each enantiomer (Boos et al., 1991; Williams and Wainer, 1999). In clinical studies, *S*-IFA was found to be more rapidly metabolized than *R*-IFA, resulting in a shorter half-life, a higher clearance and a markedly lower recovery in urine compared to *R*-IFA (Corlett et al., 1995; Wainer et al., 1996).

IFA *N*-dechloroethylation is primarily catalyzed by two major human liver P450 enzymes. CYP2B6 metabolizes *R*-IFA and *S*-IFA to produce *S*-N3-deCl-IFA and *S*-N2-deCl-IFA, respectively, whereas CYP3A4 metabolizes *R*-IFA to produce *R*-N2-deCl-IFA and *S*-IFA to yield *R*-N3-deCl-IFA (Granvil et al., 1999; Roy et al., 1999a). CYP3A4-dependent *R*-IFA 4-hydroxylation is typically more rapid than *S*-IFA 4-hydroxylation in human liver microsomes, consistent with the high level of CYP3A4 in human liver (Roy et al., 1999b), and in agreement with pharmacokinetic studies in patients (Williams and Wainer, 1999). *R*-IFA and *S*-IFA can be purified using enantioselective chromatography, and their application to clinical chemotherapy has been studied (Wainer, 1993; Wainer and Granvil, 1993). However, characterization of *R*-IFA and *S*-IFA metabolism as it impacts the anti-tumor activity of each enantiomer at the cellular level has not been investigated.

Presently, we investigate the metabolism and cytotoxicity of *R*-IFA and *S*-IFA using tumor cells engineered to express individual CYP2B and CYP3A enzymes in combination with the flavoenzyme P450 reductase (P450R). Our findings reveal that *R*-IFA displays greater cytotoxicity than either *S*-IFA or CPA toward CYP3A4-expressing tumor cells, whereas *S*-IFA displays greater activity against CYP2B-expressing tumor cells. Moreover, in vitro studies using cDNA-expressed CYPs identify the rat enzyme CYP3A1 as a superior catalyst of prodrug activation with both *R*-IFA and *S*-IFA as substrates, suggesting the utility of this P450 enzyme for gene-directed enzyme prodrug therapy involving IFA (Chen and Waxman, 2002). These findings are discussed with respect to the impact of tumor cell P450 expression on anti-tumor activity.

Materials and Methods

Materials - CPA was purchased from Sigma Chemical Co. (St. Louis, MO). CAA in the form of a 50% (w/v) solution in water, 3-aminophenol, semicarbazide and fetal bovine serum (FBS) were purchased from Aldrich Chemical Co (Milwaukee, WI). IFA was obtained from the Drug Synthesis and Chemistry Branch, National Cancer Institute (Bethesda, MD). Purified *R*-IFA and *S*-IFA were provided by Dr. Ben Skead of Cell Tech, Ltd (Cambridge, United Kingdom). 4-OOH-CPA and 4-OOH-IFA were provided by Dr. Ulf Niemeyer (Baxter Oncology GmbH, Frankfurt, Germany). Dulbecco's Modified Eagle Medium (DMEM) was purchased from

Gibco-BRL Life Technologies (Grand Island, NY). Supersomes™ containing expressed CYP2B and CYP3A enzymes, with co-expression of P450R and cytochrome b_5, were purchased from BD-Gentest Corp. (Woburn, MA). Data were obtained using the following lot numbers for each Supersome CYP preparation: 2B1, lot 5 and lot 7; 2B6, lot 8; 3A1, lot 6; 3A2, lot 6; 3A4, lot 50; 3A7, lot 1; 3A12, lot 2.

9L cell lines co-expressing P450 and P450R cDNAs - The retroviral plasmid pBabe-puro, which encodes a puromycin resistance gene, was used to clone CYP2B1 and CYP2B6 cDNAs, linked via an IRES sequence to human P450R cDNA, to give a bicistronic CYP2B-IRES-P450R expression cassette as described (Jounaidi and Waxman, 2004). The CYP2B6 cDNA used in these studies (GenBank accession no. M29874) corresponds to the wild-type (*CYP2B6**) allele, *i.e.,* Arg22/Lys139/Gln172/Ser259/Lys262/Arg487 (Lang et al., 2001). Transfection of the ecotropic packaging cell line Bosc 23 with the retroviral plasmids pBabe-CYP2B1-IRES-P450R-puro and pBabe-CYP2B6-IRES-P450R-puro, harvesting of retroviral supernatants, and infection of rat 9L gliosarcoma cells were carried out as described (Jounaidi et al., 1998), with the following modifications. Bosc 23 cells were plated at 2.5 x 10^6 cells in a 60-mm dish. Fresh culture medium (4 ml) containing chloroquine (25 μM) was added to the cells 16 h later. The cells were cotransfected 1 h later with 5 μg of retroviral plasmid DNA and 2.5 μg of the helper plasmid pKat (Finer et al., 1994) using 9 μl of the cationic liposome Fugene 6 (Boehringer-Mannheim) in a total volume of 40 μl DMEM without FBS. Pools of 9L cells resistant to 2.5 μg/ml puromycin

and expressing P450R in combination with CYP2B1 (9L/2B1-P450R cells) or CYP2B6 (9L/2B6-P450R cells) were selected beginning 48 h later over a 2–3-day period (Jounaidi and Waxman, 2004). The tumor cell line CHO, engineered to express human P450R alone (CHO/P450R cells) or P450R together with CYP3A4 (CHO/3A4-P450R cells), was that used previously (Lu and Waxman, 2005) and was kindly provided by Dr. Thomas H. Friedberg, Biomedical Research Centre, University of Dundee, UK (clonal cell line DHR/3A4) (Ding et al., 1997). The 9L and CHO tumor cells used in this study exhibit similar intrinsic sensitivities to activated CPA and IFA (see Table 1, below). Moreover, similar levels of P450 are expressed in the 9L/2B-P450R cells (Jounaidi et al., 1998) and in the CHO/3A4-P450R cells (Ding et al., 1997).

Cytotoxicity assays - The chemosensitivity of P450-expressing 9L and CHO cells was determined using a 4-day growth inhibition assay. Cells were plated in triplicate at 4000 cells per well of a 48-well plate. After 18-24 hr of growth, cells were treated for 4 days with *R*-IFA, *S*-IFA or CPA at concentrations indicated in each experiment. The same 4-day growth inhibition assay was used to evaluate the intrinsic sensitivity of the cells to CAA, a byproduct of IFA and CPA *N*-dechloroethylation, and to the 4-OOH derivatives of IFA and CPA, which decompose in aqueous medium to yield 4-OH-IFA and 4-OH-CPA, respectively. Cells were stained using a crystal violet/alcohol extraction assay and quantified. Briefly, culture dishes were washed once with phosphate-buffered saline, stained with 1.25 g crystal violet in 500 ml containing 50 ml of 37% formaldehyde and 450 ml methanol and then washed with tap water. A_{595} values were

determined using a microtiter plate reader. Background absorbance measured for wells containing culture medium alone was subtracted from each value. Data are presented as mean cell number relative to drug-free controls, with 100% growth inhibition corresponding to 0 net A_{595}, and 0% growth inhibition corresponding to the A_{595} of the drug-free control cells.

Assay for 4-OH-CPA, 4-OH-IFA and CAA released into culture medium – 9L and CHO cell lines were seeded in 12-well plates in duplicate at 1 x 10^5 cells/well in 2 ml of DMEM containing 10% FBS (9L cells) or in 2 ml of MEM containing 10% dialyzed FBS (CHO cells). Drugs were added to the cells in 2 ml of DMEM (9L cells) or MEM (CHO cells) without FBS about 20 hr later. Cells were cultured for an additional 4 hr, at which time duplicate aliquots (200 μl) of culture medium were removed. One aliquot was immediately derivatized to 1-N^6-ethenoadenosine by treatment with 20 μl of 250 mM adenosine and 30 μl of 2 M sodium acetate solution (pH 4), and then heated at 80 ^{o}C for 2.5 hr (CAA determination) (Huang and Waxman, 1999). The other aliquot was immediately derivatized to 7-hydroxyquinoline by treatment for 25 min with 100 μl of freshly prepared fluorescent reagent (60 mg of 3-aminophenol and 60 mg of hydroxylamine-HCl in 10 ml of 1N HCl) at 90^{o}C (Bohnenstengel et al., 1997). In some cases the derivatized samples were stored at -20°C in the dark prior to HPLC analysis.

Standard curves were generated using CAA (0-5 μM) and 4-OOH-CPA (0-50 μM). Standards were incubated for 2 hr with 1 x 10^5 P450-deficient 9L or CHO cells in 2 ml DMEM (pH

7.2)/well of a 12-well plate to correct for time- and cell-dependent degradation of the metabolites. The 2 hr time point corresponds to the mid-point of the standard cell culture metabolite formation assay (4 hr; see below), and serves as an estimate of the average time during which metabolites formed over the course of the 4 hr incubation period are subject to time-dependent and/or cell-dependent degradation in culture medium. The recovery of acrolein following a 2 hr incubation of 4-OOH-CPA in culture medium was 76 ± 6% (n = 2) (incubation with 9L/pBabe cells) and 89 ± 10% (n = 4) (incubation without cells). The recovery of CAA following a 2 hr incubation with and without 9L/pBabe cells was 63 ± 15% (n = 3) and 95 ± 8% (n = 3), respectively, indicating cell-dependent degradation of CAA. The accumulation of 4-OH-IFA in culture medium of 9L/2B1-P450R cells was linear with incubation times up to 8 hr, with a slope of 0.151 nmol/ml/hr per 1 x 10^5 cells seeded/well. CAA accumulation in the culture medium was linear for ~2 hr (0.164 nmol/ml/hr per 1 x 10^5 cells seeded/well), after which the rate of accumulation slowed down, consistent with the 9L cell-dependent metabolism of CAA noted above. The yields of 4-OH-IFA and CAA increased linearly with 9L/2B1-P450R cell number, with slopes of 1.37 ± 0.03 (4-OH-IFA) and 0.97 ± 0.03 (CAA) nmol metabolite/ml medium/1 x 10^5 cells seeded/well. Crystal violet absorbance values (A_{595}) were linearly correlated with cell number from 0.5 x 10^5 to 6 x 10^5 9L cells/2 ml culture medium per well of a 12-well plate. The limit of detection in culture medium (twice the background value) was 0.15 μM for CAA and 0.5 μM for acrolein.

Metabolism by cDNA-expressed CYPs – Supersomes containing baculovirus-expressed P450s (4 pmol P450) were added to 75 μl of 100 mM KPi buffer pH 7.4 containing various concentrations of *R*-IFA, *S*-IFA or CPA (50 μM to 10 mM, final substrate concentration). Assay mixtures minus NADPH were pre-incubated for 4 min at 37°C. Each reaction was initiated by addition of NADPH to 1 mM (final volume 100 μl, containing 75 mM KPi, buffer, pH 7.34, 0.75 mM EDTA and 1 mM NADPH). Reactions were incubated for 15 min at 37°C then processed and derivatized for HPLC analysis (conversion of CAA to 1-N^6-ethenoadenosine, and conversion of acrolein to 7-hydroxyquinoline) (Chen et al., 2004).

HPLC – Analysis of CPA and IFA metabolites was carried out using a Luna 5 μ C18 (2) HPLC column, 150 x 4.6 mm (Phenomenex, Torrance, CA) (Chen et al., 2004). 7-Hydroxyquinoline was eluted with 17% methanol in 0.33% phosphoric acid at a flow rate of 1 ml/min ($t_{elution}$ = 3.2 min) and was detected by fluorescence excitation at 350 nm and emission at 515 nm. 1-N^6-ethenoadenosine was eluted with 17% methanol in water ($t_{elution}$ = 7-8 min for samples incubated with cells) or 13% methanol in water ($t_{elution}$ = 8.7-10 min for Supersomes incubations) at a flow rate of 1 ml/min and was detected by fluorescence excitation at 270 nm and emission at 411 nm. Quantification was based on integrated peak areas calculated using Millennium[32] software (Waters, Inc.).

Data analysis - Data were managed using Microsoft Excel. Data based on metabolism in cell culture were corrected by subtraction of the higher of two measured background activities (culture medium from cells incubated without drugs, or from drugs incubated in medium without cells) and then converted to units of metabolite produced (nmol 7-hydroxyquinoline or nmol 1-N^6-ethenoadenosine) per A_{595} (crystal violet staining). Data obtained from in vitro metabolism assays using Supersomes were corrected by subtracting the highest of three independent background activity values: incubation without NADPH, incubation without drug and incubation without Supersomes. Data were converted to units of nmol metabolite produced/min/nmol P450. Enzyme kinetic data were analysed using Enzyme Kinetics v 0.44 software (Trinity Software, Inc.). Kinetic parameters (K_m, V_{max}) for each individual experiment, typically based on n = 7 substrate concentrations, were determined by the Eadie-Hofstee method. Mean values $\pm$ SD (n = 3) or mean values $\pm$ half the range (n = 2) were determined based on the indicated number of independent sets of assays. EC_{50} values, based on sigmoidal dose-response analysis using a variable slope, were determined using GraphPad Prism software (GraphPad Software, San Diego, CA).

Results

Metabolism of *R*-IFA, *S*-IFA and CPA by P450-expressing cell lines – The metabolism of *R*-IFA, *S*-IFA and CPA was assayed in five cell lines: 9L gliosarcoma cells expressing either rat

CYP2B1 (9L/2B1-P450R cells) or human CYP2B6 (9L/2B6-P450R cells) in combination with P450R, the P450-deficient control cell line 9L/pBabe, CHO cells expressing human CYP3A4 with P450R (CHO/3A4-P450R cells) and a control cell line expressing P450R reductase alone (CHO/P450R cells). Cells were incubated with each prodrug substrate at two concentrations (200 μM and 2 mM) and metabolites released into the culture medium were analyzed and quantified by HPLC. All three prodrugs were metabolized by the P450-expressing cell lines but not by the P450-deficient control cells (Fig. 1). CPA was primarily converted to the active, 4-OH metabolite by both CYP2B-expressing cell lines (≥98% of total metabolism) (Fig. 1A). However, this pathway corresponded to only 24-44% of CPA metabolism in the case of CYP3A4 cells, where *N*-dechloroethylation (drug inactivation) to yield CAA was the major metabolic reaction (56-76% of total metabolism) (Fig. 1B). With *R*-IFA and *S*-IFA as substrates, *N*-dechloroethylation was the major metabolic pathway for both CYP2B cell lines (up to 74% of total metabolism by 9L/2B1-P450R cells, and up to 94% of total metabolism by 9L/2B6-P450R cells. The CYP3A4 cell line showed clear enantiomeric selectivity, with up to 74% of *R*-IFA metabolism proceeding via 4-hydroxylation, as compared to 27% in the case of *S*-IFA. Moreover, the rate of *R*-IFA 4-hydroxylation by CHO/3A4-P450R cells was 1.5-fold higher than *S*-IFA 4-hydroxylation at 2 mM substrate (Fig. 1A), while the rate of *N*-dechloroethylation was 80% lower for *R*-IFA than for *S*-IFA (Fig. 1B). Overall, the rates of IFA 4-hydroxylation were much higher in the CYP3A4 cells than in either CYP2B cell line.

Cytotoxicity of *R*-IFA, *S*-IFA and CPA – The cytotoxicity of each prodrug was evaluated in each of the P450-expressing cell lines using a 4 day growth inhibition assay (Fig. 2). None of the prodrugs exerted significant cytotoxicity toward the control cell lines 9L/pBabe and CHO/P450R ('control' curves; Fig. 2), consistent with the inactivity of the parent prodrugs and the absence of oxazaphosphorine 4-hydroxylase activity in the P450-deficient cells. By contrast, all three prodrugs induced dose-dependent killing of the three P450-expressing cell lines. The rank order of cytotoxicity based on EC_{50} values (Table 1) was CPA > *S*-IFA > *R*-IFA for the CYP2B1 and CYP2B6 cells (Fig. 2A, 2B), and *R*-IFA > CPA > *S*-IFA for the CYP3A4 cells (Fig. 2C). Comparison of the activity profiles of each prodrug revealed that CPA was most cytotoxic (lowest EC_{50} value) when activated by CYP2B1 cells, whereas *R*-IFA was most active toward CYP3A4 cells. These findings are consistent with the high CPA 4-hydroxylase activity of the CYP2B1 and CYP2B6 cells, and by the high *R*-IFA 4-hydroxylase activity of the CYP3A4 cells (Fig. 1). By contrast, the CYP3A4 cells primarily metabolized *S*-IFA and CPA by N-dechloroethylation (Fig. 1). Together, these findings indicate that *R*-IFA is likely to have a better activity profile than *S*-IFA or CPA when used to treat tumors that express CYP3A4, whereas *S*-IFA is likely to be more active than *R*-IFA against tumors that express CYP2B6.

We next examined the intrinsic sensitivity of 9L cells and CHO cells to the reactive metabolites CAA, 4-OH-CPA and 4-OH-IFA, with the latter two compounds delivered to the cells as their 4-OOH derivatives (Table 1). 9L/pBabe and CHO/P450R cells both displayed high intrinsic

sensitivity to 4-OH-CPA (EC_{50} ~3 μM) and 4-OH-IFA (EC_{50} ~5 μM). Moreover, CAA was at least as cytotoxic as 4-OH-IFA (EC_{50} ~2.5-3.2 μM), suggesting that this reactive aldehyde may contribute to the cytotoxicity of IFA seen in P450 2B6 cells (Fig. 2B), which have very low IFA 4-hydroxylase activity (Fig. 1A).

Kinetic analysis of CPA and IFA metabolism by cDNA-expressed P450 enzymes – Next, we characterized the metabolic profile of the three oxazaphosphorine prodrugs using individual P450 enzymes expressed in a Baculovirus expression system ('Supersomes'). Steady-state kinetic analysis (Table 2; Fig. 3) confirmed that 4-hydroxylation was the predominant pathway of CPA metabolism catalyzed by both CYP2B enzymes. The alternative *N*-dechloroethylation pathway represented only ~ 4% of CPA metabolism in the case of CYP2B1 and was undetectable with CYP2B6 (Fig. 3B, Fig. 3C). In contrast, *R*-IFA and *S*-IFA were metabolized by CYP2B1 by both pathways, with 4-hydroxylation to *N*-dechloroethylation product ratios of ~ 1:2.2 for *R*-IFA and 1:0.8 for *S*-IFA. In the case of CYP2B6, however, IFA 4-hydroxylation was substantially reduced, in particular, in the case of the *R*-enantiomer (~3% of total metabolism). Overall, CYP2B1 metabolized all three prodrugs with an apparent K_m that was 2 to 4-fold lower than that of CYP2B6 for both metabolic pathways (Table 2). CYP2B1 and CYP2B6 were both substantially more active catalysts of CPA 4-hydroxylation than CYP3A4 (Fig. 3A and Table 2).

With CPA as substrate, CYP3A4 displayed the highest V_{max} for *N*-dechloroethylation, ~30-fold

greater than that of P450 2B1 (Table 2). By contrast, CYP3A4 metabolized *R*-IFA primarily by 4-hydroxylation, with *R*-IFA *N*-dechloroethylation corresponding to only 29% of total metabolism at V_{max}. Moreover, the V_{max} and catalytic efficiency (V_{max}/K_m) of *R*-IFA 4-hydroxylation catalyzed by CYP3A4 were 2 to 2.5-fold higher than that of CPA and *S*-IFA (Table 2 and Fig. 3A). Thus, with *R*-IFA as substrate, CYP3A4 exhibited the best kinetic profile of all three CYP enzymes, namely, high *R*-IFA 4-hydroxylase activity coupled with relatively low *N*-dechloroethylation activity, in agreement with the cell culture data presented above.

CYP3A1 is a high efficiency, low K_m catalyst of *R*-IFA and *S*-IFA 4-hydroxylation – Tumor cells may be sensitized to anti-cancer prodrugs, such as IFA, by introducing a prodrug-activating P450 gene into the tumor, which thereby acquires the capacity for localized prodrug activation (Chen and Waxman, 2002). Thus, CYP3A4 can be used to sensitize P450-deficient tumor cells to the cytotoxic activity of IFA (Jounaidi et al., 1998). Presently, we considered the possibility that other CYP3A enzymes might metabolize one of the enantiomers of IFA with improved activity or catalytic specificity compared to CYP3A4. Table 3 and Fig. 3 present the steady-state kinetic parameters determined for metabolism of CPA, *R*-IFA and *S*-IFA by four other cDNA-expressed CYP3A enzymes: rat CYP3A1, rat CYP3A2, human CYP3A7 and dog CYP3A12. All four CYP3A enzymes preferentially metabolized *R*-IFA by the 4-hydroxylation pathway, to an even greater extent than seen with CYP3A4 (up to 90% of total metabolism; Fig. 3C). CPA was preferentially metabolized by *N*-dechloroethylation by all of the CYP3A enzymes except

CYP3A7, which was primarily a 4-hydroxylase with CPA and with both enantiomers of IFA. However, the overall catalytic efficiency of CYP3A7 for oxazaphosphorine activation was greatly reduced by this enzyme's low intrinsic catalytic activity (V_{max} ~10-28% that of CYP3A4; Table 3 vs. Table 2). CYP3A12 preferentially metabolized *S*-IFA via *N*-dechloroethylation, as seen with CYP3A4, whereas CYP3A1, CYP3A2 and CYP3A7 metabolized *S*-IFA preferentially by 4-hydroxylation (Fig. 3C). Finally, CYP3A1 displayed K_m values for *R*- and *S*-IFA 4-hydroxylation of ~200 μM (Table 3), ~4-5-fold lower than the corresponding K_m values of CYP3A4 (Table 2). The high catalytic efficiency of CYP3A1 for *R*-IFA and *S*-IFA 4-hydroxylation (V_{max}/K_m = 88-135 mol/min/mol P450/μM) compared to six other CYP enzymes (Fig. 3A), coupled with CYP3A1's low K_m and its low relative rate of *N*-dechloroethylation (Fig. 3C) evidence the superior catalytic properties of this enzyme for IFA activation.

Discussion

The anti-cancer prodrugs CPA and IFA are well established to be actively metabolized in the liver, which is a major determinant of the pharmacokinetics of prodrug activation and the rate of drug inactivation and elimination from the body. More recent studies have shown that tumor cells also express drug-metabolizing P450 enzymes, including CYP2B6 (Nakajima et al., 1996; Standop et al., 2003) and CYP3A4 (Huang et al., 1996; Murray et al., 1999; Schmidt et al., 2004). The levels of tumor cell P450 are low, but may nevertheless be an important factor in the metabolism and activity of these anti-cancer agents. Tumor cell-expressed P450 enzymes may potentially contribute to drug inactivation leading to drug resistance, in the case of anti-cancer drugs than are inactivated by P450 metabolism, and conversely, may enhance anti-tumor activity in the case of P450 prodrugs, as demonstrated for CPA and IFA in cultured tumor cells and in tumor xenograft models in vivo (Chen and Waxman, 1995). The studies presented here investigate the metabolism and cytotoxicity of *R*-IFA, *S*-IFA and CPA in tumor cells engineered to express individual CYP2B and CYP3A enzymes with the goal of identifying P450 prodrug–P450 enzyme combinations that are associated with strong cytotoxic responses. Our findings reveal that tumor cells that express CYP3A4 are most sensitive to the cytotoxicity of *R*-IFA, whereas tumor cells that express CYP2B enzymes (rat CYP2B1 or human CYP2B6) are most sensitive to CPA. Moreover, the combination of *R*-IFA treatment with CYP3A4 expression was associated with favorable partitioning of IFA metabolism along the

therapeutically important 4-hydroxylation (prodrug activation) pathway at the expense of the alternative, *N*-dechloroethylation pathway, which inactivates the prodrug and yields the by-product CAA, which has been linked to undesirable host toxicities, notably neurotoxicity and urotoxicity. Together, these findings suggest that improvement in the effectiveness of oxazaphoshorine therapy may be achieved by individualizing drug treatment based on the P450 expression profile of each patient's tumor, e.g., as assessed by needle biopsy.

Studies using cDNA-expressed enzymes revealed that CPA 4-hydroxylation was most actively catalyzed by CYP2B1 and CYP2B6, with little (CYP2B1) or no (CYP2B6) *N*-dechloroethylation activity detected. The overall catalytic efficiency (V_{max}/K_m) was highest with CYP2B1, largely due to its ~3-fold lower K_m for CPA, and this translated into a 2-fold increase in cytotoxicity compared to CYP2B6, as indicated by EC_{50} values (Table 1). CYP3A4 preferentially metabolized CPA by *N*-dechloroethylation (~75% of total metabolism), with the catalytic efficiency for the 4-hydroxylation reaction being only 15-30% that of CYP2B1 and CYP2B6 (Fig. 3A). However, with *R*-IFA as substrate, CYP3A4 exhibited high 4-hydroxylase activity coupled with a comparatively low *N*-dechloroethylation activity. CYP3A4 is a major catalyst of IFA metabolism in human liver microsomes (Chang et al., 1993; Walker et al., 1994) and the most abundant cytochrome P450 enzyme in human liver. The present findings suggest that the anti-cancer activity of racemic IFA, as used in the clinic, is in large part be due to *R*-IFA, insofar as *S*-IFA is primarily metabolized by *N*-dechloroethylation, catalyzed by CYP3A4 and CYP2B6 (Fig. 3C). These findings support the use of *R*-IFA in place of racemic IFA or its *S*-enantiomer, as

proposed by Wainer and associates (Williams and Wainer, 1999) based on the more extensive 4-hydroxylation of *R*-IFA than *S*-IFA seen in pharmacokinetic studies (Wainer et al., 1994) and by the finding that the *N*-dechloroethylation of *R*-IFA is less extensive than that of *S*-IFA in incubations with human liver microsomes (Roy et al., 1999a).

CYP3A4 can be used in a P450-based enzyme prodrug therapy to sensitize tumor cells to racemic IFA and, to a lesser extent, CPA (Jounaidi et al., 1998). Analysis of *R*-IFA and *S*-IFA metabolism catalyzed by a panel of cDNA-expressed CYP3A enzymes revealed that the rat enzyme CYP3A1 exhibits superior catalytic activity compared to four other CYP3A enzymes, including CYP3A4. CYP3A1 exhibited high intrinsic 4-hydroxylase activity, minimal *N*-dechloroethylation activity (11% of total metabolism at V_{max}) and a comparatively low K_m compared to the other CYP3A enzymes examined, indicating that this P450 may be useful in combination with *R*-IFA or *S*-IFA in clinical trials of this P450-based cancer therapy (Lohr et al., 2003; Braybrooke et al., 2005). CYP3A12, which is expressed in dog liver, exhibited a preferential 4-hydroxylation of *R*-IFA compared to *S*-IFA, however, CYP3A12 suffered from a high K_m and low catalytic efficiency for *R*-IFA 4-hydroxylation compared to CYP3A1. CYP3A5, like CYP3A4, also exhibits a preference for 4-hydroxylation of *R*-IFA compared with *S*-IFA (Roy et al., 1999a). Another human liver enzyme, CYP3A7, exhibited the lowest catalytic activity of all five CYP3A enzymes toward both enantiomers of IFA.

CAA, a byproduct of oxazaphosphorine metabolism, displayed appreciable cytotoxic activity in cell culture (EC_{50} ~ 2.5 μM, compared to EC_{50} values of 3-5 μM for the 4-hydroxy derivatives of CPA and IFA; Table 1), in agreement with earlier studies in various tumor cell lines (Brueggemann et al., 2002). However, CAA is not generally regarded as an active, therapeutic metabolite of IFA or CPA. CAA exhibits some anti-tumor activity in vivo, albeit substantially less than that of 4-OH-IFA (Borner et al., 2000). Of note, we observed that the rate of 4-hydroxylation of *R*-IFA by CYP2B6-expressing 9L gliosarcoma cells was 5-fold lower than that of 9L cells expressing CYP2B1, yet in growth inhibition assays the CYP2B6 cells showed sensitivity to *R*-IFA comparable to that of CYP2B1 cells. This discrepancy suggests that at least a portion of the cytotoxic activity of *R*-IFA (and also *S*-IFA) is due to the formation of CAA via *N*-dechloroethylation in the case of the CYP2B6 cells.

Given the host toxicities that are widely believed to be linked to CAA exposure, decreasing *N*-dechloroethylation through the use of *R*-IFA may result in an increase in therapeutic index. Further study is required to determine whether *R*-IFA treatment in vivo leads to enhanced *R*-IFA metabolism ('autoinduction'), via increased expression of CYP3A4 (Chang et al., 1997), as has been seen with racemic IFA (Kerbusch et al., 2001). It will also be important to determine whether *R*-IFA treatment is associated with anti-angiogenic activity similar to that seen when CPA is administered repeatedly in low doses using metronomic (Man et al., 2002) or anti-angiogenic treatment schedules (Browder et al., 2000). This latter approach is highly effective

when applied to CPA in the context of prodrug-activation gene therapy using CYP2B6 (Jounaidi and Waxman, 2001). Based on the present findings, this latter strategy may also be implemented by targeted delivery of CYP3A1 to tumors *in situ* in combination with *R*-IFA treatment. The low K_m for IFA exhibited by CYP3A1 compared to CYP3A4 may provide the opportunity to shift prodrug activation from the liver to the tumor, thereby increasing the anti-tumor effect and potentially reducing host toxicity.

Footnotes: *Supported in part by NIH grant CA49248 (to D.J.W.)

References

Bohnenstengel F, Eichelbaum M, Golbs E and Kroemer HK (1997) High-performance liquid chromatographic determination of acrolein as a marker for cyclophosphamide bioactivation in human liver microsomes. *J Chromatogr B Biomed Sci Appl.* **692:**163-168.

Boos J, Welslau U, Ritter J, Blaschke G and Schellong G (1991) Urinary excretion of the enantiomers of ifosfamide and its inactive metabolites in children. *Cancer Chemother Pharmacol* **28:**455-460.

Borner K, Kisro J, Bruggemann SK, Hagenah W, Peters SO and Wagner T (2000) Metabolism of ifosfamide to chloroacetaldehyde contributes to antitumor activity in vivo. *Drug Metab Dispos.* **28:**573-576.

Braybrooke JP, Slade A, Deplanque G, Harrop R, Madhusudan S, Forster MD, Gibson R, Makris A, Talbot DC, Steiner J, White L, Kan O, Naylor S, Carroll MW, Kingsman SM and Harris AL (2005) Phase I study of MetXia-P450 gene therapy and oral cyclophosphamide for patients with advanced breast cancer or melanoma. *Clin Cancer Res* **11:**1512-1520.

Browder T, Butterfield CE, Kraling BM, Shi B, Marshall B, O'Reilly MS and Folkman J (2000) Antiangiogenic scheduling of chemotherapy improves efficacy against experimental drug-resistant cancer. *Cancer Res* **60:**1878-1886.

Brueggemann SK, Schlenke P, Klich S, Deeken M, Peters SO and Wagner T (2002) Stem cell toxicity of oxazaphosphorine metabolites in comparison to their antileukemic activity. *Biochem Pharmacol* **63:**1337-1341.

Chang TK, Yu L, Maurel P and Waxman DJ (1997) Enhanced cyclophosphamide and ifosfamide activation in primary human hepatocyte cultures: response to cytochrome P-450 inducers and autoinduction by oxazaphosphorines. *Cancer Res* **57:**1946-1954.

Chang TKH, Weber GF, Crespi CL and Waxman DJ (1993) Differential activation of cyclophosphamide and ifosphamide by cytochromes P450 2B and 3A in human liver microsomes. *Cancer Res.* **53:**5629-5637.

Chen CS, Lin JT, Goss KA, He YA, Halpert JR and Waxman DJ (2004) Activation of the anticancer prodrugs cyclophosphamide and ifosfamide: identification of cytochrome P450 2B enzymes and site-specific mutants with improved enzyme kinetics. *Mol Pharmacol* **65:**1278-1285.

Chen L and Waxman DJ (1995) Intratumoral activation and enhanced chemotherapeutic effect of oxazaphosphorines following cytochrome P450 gene transfer: development of a combined chemotherapy/cancer gene therapy strategy. *Cancer Res* **55:**581-589.

Chen L and Waxman DJ (2002) Cytochrome P450 gene-directed enzyme prodrug therapy (GDEPT) for cancer. *Curr Pharm Des* **8:**1405-1416.

Corlett SA, Parker D and Chrystyn H (1995) Pharmacokinetics of ifosfamide and its enantiomers following a single 1 h intravenous infusion of the racemate in patients with small cell lung

carcinoma. *Br J Clin Pharmacol* **39:**452-455.

Ding S, Yao D, Burchell B, Wolf CR and Friedberg T (1997) High levels of recombinant CYP3A4 expression in Chinese hamster ovary cells are modulated by coexpressed human P450 reductase and hemin supplementation. *Arch Biochem Biophys* **348:**403-410.

Finer MH, Dull TJ, Qin L, Farson D and Roberts MR (1994) kat: a high-efficiency retroviral transduction system for primary human T lymphocytes. *Blood* **83:**43-50.

Granvil CP, Madan A, Sharkawi M, Parkinson A and Wainer IW (1999) Role of CYP2B6 and CYP3A4 in the in vitro N-dechloroethylation of (R)- and (S)-ifosfamide in human liver microsomes. *Drug Metab Dispos.* **27:**533-541.

Huang Z, Fasco MJ, Figge HL, Keyomarsi K and Kaminsky LS (1996) Expression of cytochromes P450 in human breast tissue and tumors. *Drug Metab Dispos* **24:**899-905.

Huang Z and Waxman DJ (1999) High-performance liquid chromatographic-fluorescent method to determine chloroacetaldehyde, a neurotoxic metabolite of the anticancer drug ifosfamide, in plasma and in liver microsomal incubations. *Anal Biochem* **273:**117-125.

Jounaidi Y, Hecht JED and Waxman DJ (1998) Retroviral transfer of human cytochrome P450 genes for oxazaphosphorine-based cancer gene therapy. *Cancer Res.* **58:**4391-4401.

Jounaidi Y and Waxman DJ (2001) Frequent, moderate-dose cyclophosphamide administration improves the efficacy of cytochrome P-450/cytochrome P-450 reductase-based cancer gene therapy. *Cancer Res* **61:**4437-4444.

Jounaidi Y and Waxman DJ (2004) Use of replication-conditional adenovirus as a helper system to enhance delivery of P450 prodrug-activation genes for cancer therapy. *Cancer Res* **64:**292-303.

Kerbusch T, Mathot RA, Keizer HJ, Kaijser GP, Schellens JH and Beijnen JH (2001) Influence of dose and infusion duration on pharmacokinetics of ifosfamide and metabolites. *Drug Metab Dispos* **29:**967-975.

Lang T, Klein K, Fischer J, Nussler AK, Neuhaus P, Hofmann U, Eichelbaum M, Schwab M and Zanger UM (2001) Extensive genetic polymorphism in the human CYP2B6 gene with impact on expression and function in human liver. *Pharmacogenetics* **11:**399-415.

Lohr M, Kroger J-C, Hoffmeyer A, Freund M, Hain J, Holle A, Knofel WT, Liebe S, Nizze H, Renner M, Saller R, Muller P, Wagner T, Hauenstein K, Salmons B and Gunzburg WH (2003) Safety, feasibility and clinical enefit of localized chemotherapy using microencapsulated cells for inoperatble pancreatic carcinoma in a phase I/II trial. *Cancer Therapy* **1:**121-131.

Lu H and Waxman DJ (2005) Anti-tumor activity of methoxymorpholinyl doxorubicin: potentiation by cytochrome P450 3A metabolism. *Mol Pharmacol* **67:**212-219.

Man S, Bocci G, Francia G, Green SK, Jothy S, Hanahan D, Bohlen P, Hicklin DJ, Bergers G and Kerbel RS (2002) Antitumor effects in mice of low-dose (metronomic) cyclophosphamide administered continuously through the drinking water. *Cancer Res* **62:**2731-2735.

Murray GI, McFadyen MC, Mitchell RT, Cheung YL, Kerr AC and Melvin WT (1999) Cytochrome P450 CYP3A in human renal cell cancer. *Br J Cancer* **79:**1836-1842.

Nakajima T, Wang RS, Nimura Y, Pin YM, He M, Vainio H, Murayama N, Aoyama T and Iida F (1996) Expression of cytochrome P450s and glutathione S-transferases in human esophagus with squamous-cell carcinomas. *Carcinogenesis* **17:**1477-1481.

Roy P, Tretyakov O, Wright J and Waxman DJ (1999a) Stereoselective metabolism of ifosfamide by human P-450s 3A4 and 2B6. Favorable metabolic properties of R-enantiomer. *Drug Metab Dispos* **27:**1309-1318.

Roy P, Yu LJ, Crespi CL and Waxman DJ (1999b) Development of a substrate-activity based approach to identify the major human liver P450 catalysts of cyclophosphamide and ifosfamide activation based on cDNA-expressed activities and liver microsomal P450 profiles. *Drug Metab Dispos.* **27:**655-666.

Schmidt R, Baumann F, Knupfer H, Brauckhoff M, Horn LC, Schonfelder M, Kohler U and Preiss R (2004) CYP3A4, CYP2C9 and CYP2B6 expression and ifosfamide turnover in breast cancer tissue microsomes. *Br J Cancer* **90:**911-916.

Sladek NE (1988) Metabolism of oxazaphosphorines. *Pharmacol Ther.* **37:**301-355.

Standop J, Schneider M, Ulrich A, Buchler MW and Pour PM (2003) Differences in immunohistochemical expression of xenobiotic-metabolizing enzymes between normal pancreas, chronic pancreatitis and pancreatic cancer. *Toxicol Pathol* **31:**506-513.

Wainer IW (1993) Stereoisomers in clinical oncology: why it is important to know what the right and left hands are doing. *Ann Oncol* **4 Suppl 2:**7-13.

Wainer IW, Ducharme J and Granvil CP (1996) The N-dechloroethylation of ifosfamide: using stereochemistry to obtain an accurate picture of a clinically relevant metabolic pathway. *Cancer Chemother Pharmacol.* **37:**332-336.

Wainer IW and Granvil CP (1993) Stereoselective separations of chiral anticancer drugs and their application to pharmacodynamic and pharmacokinetic studies. *Ther Drug Monit* **15:**570-575.

Wainer IW, Granvil CP, Wang T and Batist G (1994) Efficacy and toxicity of ifosfamide stereoisomers in an in vivo rat mammary carcinoma model. *Cancer Res* **54:**4393-4397.

Walker D, Flinois JP, Monkman SC, Beloc C, Boddy AV, Cholerton S, Daly AK, Lind MJ, Pearson AD, Beaune PH and et al. (1994) Identification of the major human hepatic cytochrome P450 involved in activation and N-dechloroethylation of ifosfamide. *Biochem Pharmacol* **47:**1157-1163.

Williams ML and Wainer IW (1999) Cyclophosphamide versus ifosfamide: to use ifosfamide or not to use, that is the three-dimensional question. *Curr Pharm Des* **5:**665-672.

Woodland C, Ito S, Granvil CP, Wainer IW, Klein J and Koren G (2000) Evidence of renal metabolism of ifosfamide to nephrotoxic metabolites. *Life Sci* **68:**109-117.

Zalupski M and Baker LH (1988) Ifosfamide. *J Natl Cancer Inst.* **80:**556-566.

Figure Legends

Figure 1 - Metabolism of CPA, *R*-IFA and *S*-IFA by 9L/2B1-P450R, 9L/2B6-P450R and CHO/3A4-P450R cells by 4-hydroxylation (A) and by *N*-dechloroethylation (B). Cell lines expressing the indicated P450s in combination with P450R were cultured in 12-well plates and incubated for 4 hr with each prodrug substrate at 0.2 or 2.0 mM, followed by metabolite derivatization and HPLC analysis. Data were quantified by comparison to standard curves prepared using metabolite standards (4-OOH-CPA or CAA) incubated with P450-deficient cells, as described in Materials and Methods. Data shown are rates of metabolite production over a 4 hr period, expressed as nmol metabolite per well, normalized for the cell density of each culture well (A_{595}; crystal violet staining intensity) (mean values $\pm$ half the range for duplicate determinations). 9L, 9L/pBabe cells; CHO, CHO/P450R cells; *, metabolite is below limit of detection.

Figure 2 – Growth inhibitory effects of CPA, *R*-IFA and *S*-IFA toward P450-expressing cell lines. The cytotoxicity of each prodrug was assayed in a 4-day growth inhibition assay carried out using 9L/2B1-P450R cells (A), 9L/2B6-P450R cells (B) and CHO/3A4-P450R cells (C) in comparison to a P450-deficient control cell line ('control': 9L/pBabe for panels A and B, CHO/P450R for panel C; control data presented are mean $\pm$ SD values for n =3 separate incubations carried out with each prodrug). Cells were seeded in 48-well plates at 4000 cells/well

and treated with increasing concentrations of each prodrug (0 to 1 mM, n=8 concentrations, each done in triplicate) for 4 days as described in Materials and Methods. Data presented are mean ± half-the-range values, with the growth inhibition of the drug-free controls set to 0 (duplicate experiments with n = 3 replicates each).

Figure 3 – Catalytic efficiencies for metabolism of CPA, *R*-IFA and *S*-IFA by CYP2B and CYP3A enzymes and percent metabolism via N-dechloroethylation. Data shown are based on the steady-state kinetic analyses determined for the indicated seven cDNA-expressed P450 enzymes and summarized in Tables 2 and 3. Data shown are V_{max}/K_m values determined by Eadie-Hofstee analysis (mean ± half-the-range for n = 2-3 independent sets of determinations) for 4-hydroxylation (A) and N-dechloroethylation (B) of each prodrug substrate. V_{max}/K_m values are in units of mol product/min/mol P450/mM. Panel C, percent of total metabolism proceeding via N-dechloroethylation pathway, calculated based on the V_{max} values for each enzyme and the metabolic profiles shown in Tables 2 and 3. *, metabolite is below the limit of detection.

DMD Fast Forward. Published on May 26, 2005 as DOI: 10.1124/dmd.105.004788
This article has not been copyedited and formatted. The final version may differ from this version.

Table 1 – Cytotoxicity of anti-cancer prodrugs and their metabolites toward P450-expressing 9L and CHO cells[a]

	9L/pBabe	CHO/HR	9L/2B1	9L/2B6	CHO/3A4
	EC_{50} (μM)				
CPA	ND[b]	ND	54.8	105.4	88.7
R-IFA	ND	ND	294.8	220.1	57.9
S-IFA	ND	ND	91.9	110.6	125.6
4OOH-CPA	3.0	3.2	-[c]	-	-
4OOH-IFA	5.1	5.0	-	-	-
CAA	3.2	2.5	-	-	-

Notes:

a - Data are mean values based on two independent sets of 4-day cytotoxicity assays for each cell line. EC_{50} values were calculated using sigmoidal dose-response (variable slope) method of GraphPad Prism software.

b - ND, not detectable, indicating ≤ 20% toxicity observed at the highest drug concentration tested

c - ‘ - ‘, not investigated

DMD Fast Forward. Published on May 26, 2005 as DOI: 10.1124/dmd.105.004788
This article has not been copyedited and formatted. The final version may differ from this version.

Table 2 - Steady-state kinetics analysis: CPA, *R*-IFA and *S*-IFA metabolism by cDNA-expressed CYPs 2B1, 2B6 and 3A4. Data shown are mean ± SD values based on n=3 independent determinations. ND, not determined due to low activity.

P450	Prodrug	4-Hydroxylation		N-Dechloroethylation	
		K_m (mM)	V_{max} (mol/min/ mol P450)	K_m (mM)	V_{max} (mol/min/ mol P450)
2B1	CPA	0.40 ± 0.06	73.5 ± 7.5	0.55 ± 0.13	3.0 ± 0.7
	R-IFA	0.54 ± 0.10	19.0 ± 1.5	0.70 ± 0.22	43.6 ± 14.5
	S-IFA	0.56 ± 0.06	32.2 ± 1.4	0.69 ± 0.04	27.2 ± 6.4
2B6	CPA	1.33 ± 0.04	123.2 ± 5.5	ND	0
	R-IFA	2.24 ± 1.15	1.98 ± 0.6	1.42 ± 0.38	62.3 ± 3.8
	S-IFA	1.27 ± 0.24	17.1 ± 2.8	1.24 ± 0.20	58.3 ± 4.2
3A4	CPA	1.13 ± 0.22	31.9 ± 4.9	1.61 ± 0.22	94.2 ± 9.1
	R-IFA	0.98 ± 1.14	63.7 ± 7.2	1.10 ± 0.27	26.0 ± 5.7
	S-IFA	0.99 ± 0.24	25.0±2.4	1.50 ± 0.30	125 ± 23

DMD Fast Forward. Published on May 26, 2005 as DOI: 10.1124/dmd.105.004788
This article has not been copyedited and formatted. The final version may differ from this version.

Table 3 - Steady-state kinetics analysis: CPA, *R*-IFA and *S*-IFA metabolism by cDNA-expressed CYPs 3A1, 3A2, 3A7 and 3A12. Data based on two independent determinations (mean values ± half-the-range).

P450	Drug	4-Hydroxylation		N-Dechloroethylation	
		K_m (mM)	V_{max} (mol/min/ mol P450)	K_m (mM)	V_{max} (mol/min/ mol P450)
3A1	CPA	1.15 ± 0.28	10.5 ± 0.5	0.69 ± 0.24	25.5 ± 2.7
	R-IFA	0.22 ± 0.04	19.3 ± 0.5	0.61 ± 0.16	2.5 ± 0.5
	S-IFA	0.19 ± 0.03	23.1 ± 2.2	0.36 ± 0.10	2.9 ± 0.2
3A2	CPA	1.82 ± 0.34	8.5 ± 0.7	1.97 ± 0.12	28.4 ± 3.8
	R-IFA	0.95 ± 0.12	23.9 ± 0.4	1.19 ± 0.09	3.4 ± 0.9
	S-IFA	1.10 ± 0.13	21.2± 0.8	1.17 ± 0.06	12.5 ± 4.2
3A7	CPA	1.04 ± 0.01	8.8 ± 1.8	2.03 ± 0.74	1.6 ± 0.6
	R-IFA	1.05 ± 0.05	6.0 ± 2.3	3.41 ± 1.88	1.1 ± 0.3
	S-IFA	0.42 ± 0.02	4.4 ± 1.8	0.57 ± 0.22	1.3 ± 0.4
3A12	CPA	3.42 ± 0.37	24.2 ± 4.8	6.78 ± 0.70	55.8 ± 18.6
	R-IFA	1.83 ± 0.21	32.5 ± 8.9	5.78 ± 1.33	8.5 ± 5.0
	S-IFA	0.92 ± 0.08	14.3 ± 1.4	2.89 ± 0.84	49.4 ± 19.7

DMD Fast Forward. Published on May 26, 2005 as DOI: 10.1124/dmd.105.004788
This article has not been copyedited and formatted. The final version may differ from this version.

Fig. 1

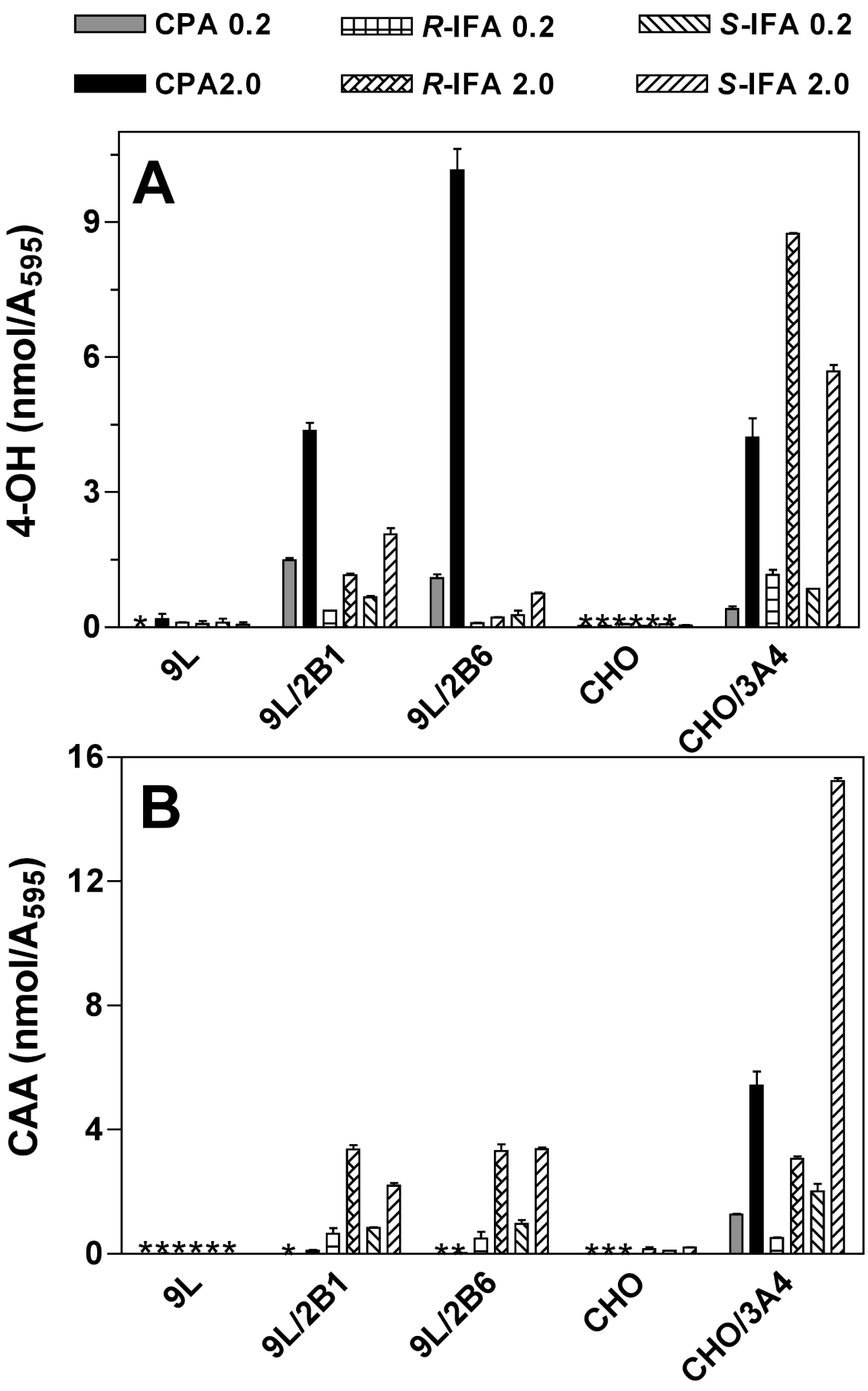

DMD Fast Forward. Published on May 26, 2005 as DOI: 10.1124/dmd.105.004788
This article has not been copyedited and formatted. The final version may differ from this version.

Fig. 2

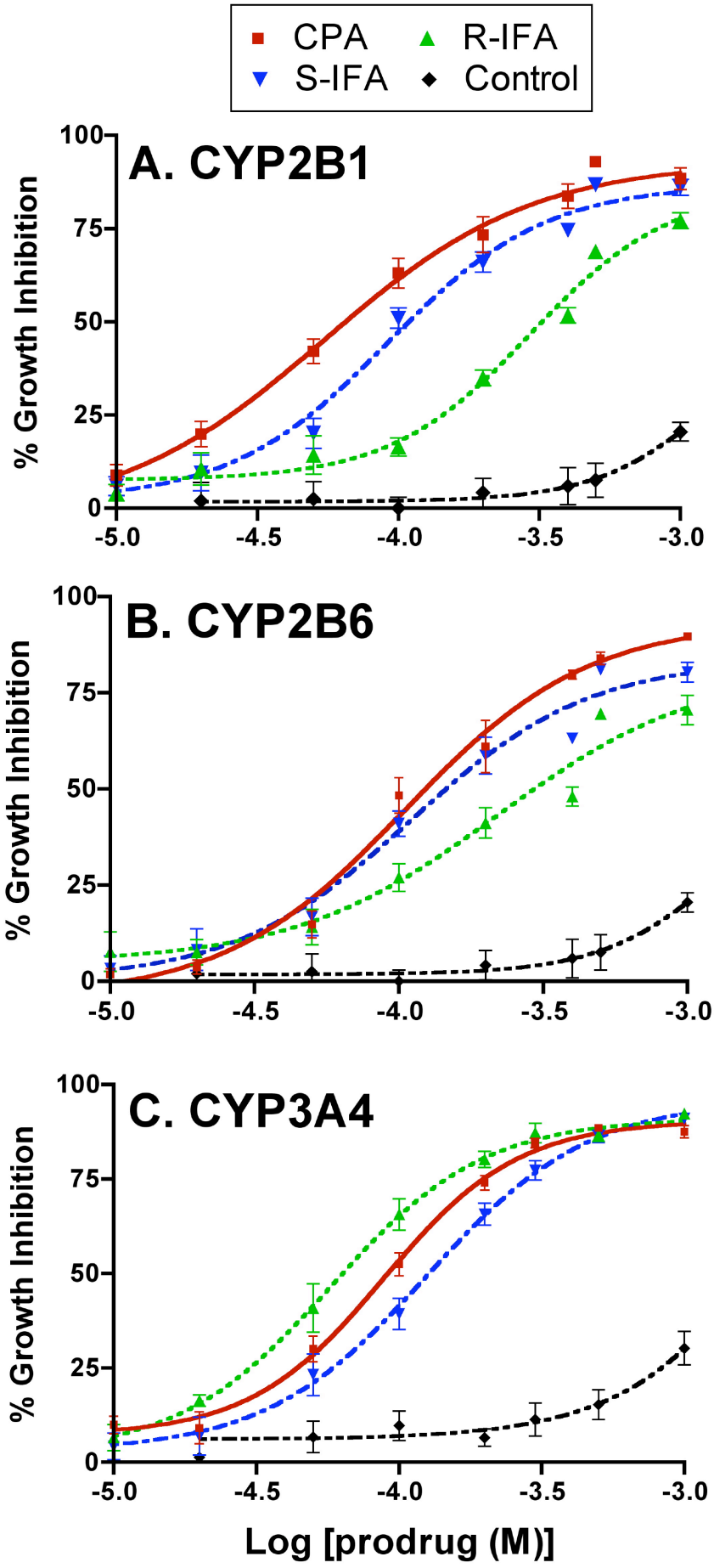

DMD Fast Forward. Published on May 26, 2005 as DOI: 10.1124/dmd.105.004788
This article has not been copyedited and formatted. The final version may differ from this version.

Fig. 3